Novel Phased Array Scanning Employing A Single Feed Without Using Individual Phase Shifters

Nicholas K. Host, Chi-Chih Chen, and John L. Volakis
The ElectroScience Laboratory, The Ohio State University,
1330 Kinnear Road
Columbus, OH 43212

Félix A. Miranda
NASA Glenn Research Center
12000 Brookpark Road
Cleveland, OH 44135

ABSTRACT

Phased arrays afford many advantages over mechanically steered systems. However, they are also more complex, heavy, and most of all costly. The high cost mainly originates from the complex feeding structure. This paper proposes a novel feeding scheme to eliminate all phase shifters and achieve scanning via one-dimensional motion. Beam scanning is achieved via a series fed array incorporating feeding transmission lines whose wave velocity can be mechanically adjusted. Along with the line design, ideal element impedances to be used in conjunction with the line are derived. Practical designs are shown which achieve scanning to ±30º from boresight. Finally, a prototype is fabricated and measured, demonstrating the concept.

Keywords: Dipole, parallel plate transmission line, phased array feeding, series fed array

1.0 Introduction

Phased array systems provide advantages over mechanically steered systems for their conformality, high aperture efficiency, and unfettered beam steering. However, this advancement in capability comes at the price of complexity, weight, and cost. The major source of these complications arises from the backend manifold where a complex feeding network is required to induce scanning. To address these issues, this paper proposes a novel feeding approach to eliminate the need for a complicated backend. Specifically, a series fed array employing a wave velocity reconfigurable transmission line is used to achieve scanning. The wave velocity will be reconfigured for the entire array with one mechanical motion to change the progressive phase delivered to each element. In this way, scanning will be accomplished using only one feed and no individual phase shifters.

Phased arrays are typically fed in one of two ways. The first and more prevalent method is the corporate feed (see [1]). In this method, power is branched out from the source to each element. The second method is a serial feed as in [2]. For this method, each antenna element is fed by an individual feed that taps off the central feedline. Both methods rely on the use of phase shifters at each element to steer the beam. Thus, as the array gets larger, these approaches become cumbersome and very expensive. Treatments to the array are commonly used to lower the cost. One such treatment is array thinning as seen in [3]. This reduces the number of elements, even below the Nyquist sampling rate. Even with advanced algorithms, pattern degradation does occur. Most notably, the directivity can be severely lowered. Another treatment is to employ subarrays as in [4]. In this approach, a single phase shifter is used to feed multiple elements (called a subarray) in an effort to reduce the total number of phase shifters. However, this approach also leads to degraded patterns and directivity.

In our design, we eliminate the need for phase shifters and instead mechanically modify the transmission line for phase shifting. A similar concept is seen in [5]. In [5], a nonfoster circuit is used at each element to realize true time delay at the expense of complexity and cost. In contrast, our approach controls all transmission line segments with one mechanical movement. Furthermore, our transmission line could be used in a true time delay operation mode since it is nondispersive in nature. However, the layout would have to be closer to a corporate feed. Accordingly, we chose to stay with a serial feed configuration due to its compactness.

2. Transmission Line

The most important part of the concept is the transmission line design. Two dielectric sheets house one plate of the transmission line and one dipole arm (see Figure 1). Each element is connected in series via the wave velocity

reconfigurable transmission line pictured in Figure 2. The transmission line is parallel plate line, partially filled with dielectric. The wave velocity of the supported wave is determined by the ratio of dielectric to air. Thus, the velocity can be controlled by adjusting the spacing between the two plates. Scanning is then achieved by mechanically moving the top plate to adjust the line's wave velocity and therefore the progressive phase delivered to each element. We remark that the line impedance will also change with this mechanical movement. This will be discussed in section III and will also be the source of future research.

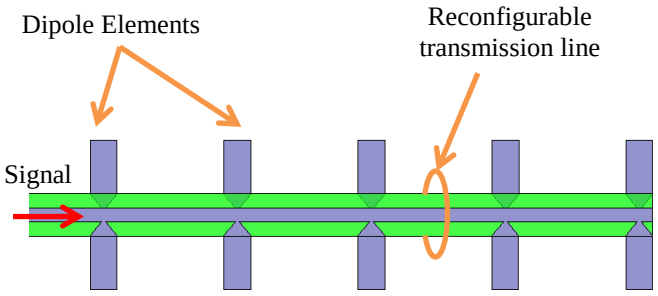

Figure 1 - Proposed phased array feeding scheme

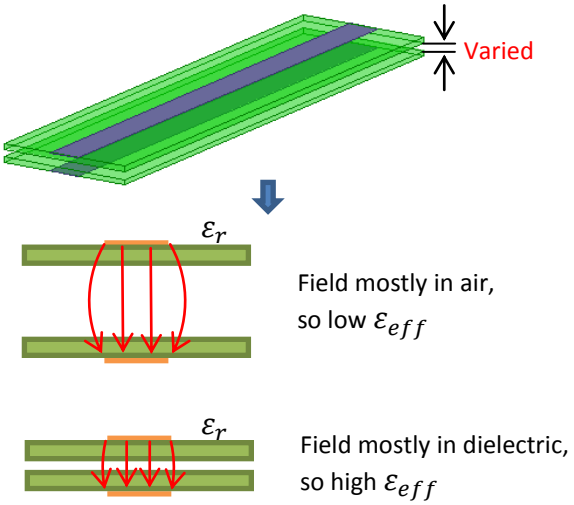

Figure 2 - Wave velocity reconfigurable transmission line (top) in two different spacing configurations: Spread far apart (middle) to achieve a low effective permittivity and close together (bottom) to achieve a high effective permittivity

The scan angle achieved depends on the element spacing and the supported wave velocity (or similarly propagation constant). Figure 3 shows the scan angle for a given propagation constant and element spacings. Note that scan angles greater than 60º from boresight have been omitted for clarity (since they are very close together). Also note that the propagation constant is given as a normalized propagation constant $\left(k_{eff}/k_0 = \sqrt{\varepsilon_{eff}\mu_{eff}} \cong \sqrt{\varepsilon_{eff}}\right)$. In effect, the chart gives insight into the requirements for the transmission line. One can see that for an element spacing of $\lambda/2$ and a $k_{eff}/k_0 = 2$, the array will scan to boresight. Additionally, one can see that for a scan range between -60º and 60º and an element spacing of $\lambda/4$, the line would need to achieve $3 \leq k_{eff}/k_0 \leq 4.7$.

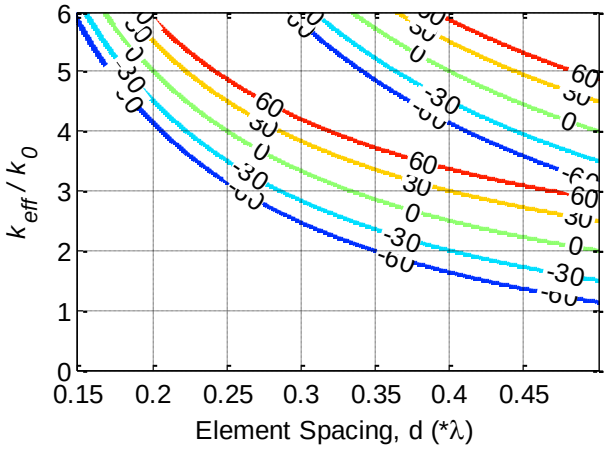

Figure 3 - Scan angle from boresight as a function of propagation constant and element spacing

The transmission line parameters at issue are depicted in Figure 4. In this case a dielectric constant of $\varepsilon_r = 25$ was selected while two different dielectric thicknesses were simulated. Figure 5 shows the k_{eff}/k_0 as the air gap, g, is varied. From this data we observe that the maximum k_{eff}/k_0 is approximately the same for both thicknesses. This occurs when there is no air gap and the top and bottom dielectrics are touching. k_{eff}/k_0 is a little under 5 as expected since the dielectric constant being used is 25 and $k_{eff}/k_0 \cong \sqrt{\varepsilon_{eff}}$. k_{eff}/k_0 being less than 5 is expected since the fringe fields are not completely contained between the plates; some fields will go outward into the air before reaching the opposite conductor. The permittivity of the dielectric then determines the upper bound for k_{eff}/k_0.

As the plates are separated, k_{eff}/k_0 is determined by the ratio of the dielectric and air thickness forming the transmission line. Typically, we choose thinner dielectric since the k_{eff}/k_0 drops faster as the plates' dielectrics are separated. Note, the plates must be kept close enough to keep the line in transmission line mode, otherwise the lines will radiate. The lower bound is then determined by the distance that the transmission line plates can be separated. This leads to another advantage for thinner lines since they can have a larger air gap before exiting

transmission line mode. Figure 6 shows the possible scan angles achievable for two different dielectric thicknesses.

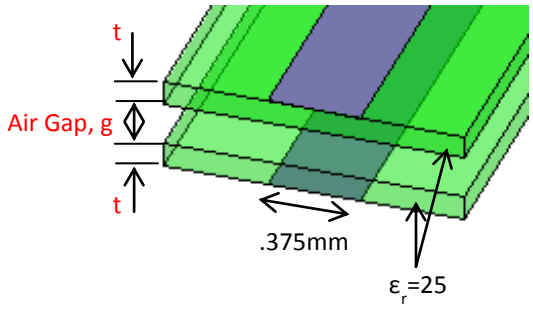

Figure 4 - Sample transmission line design

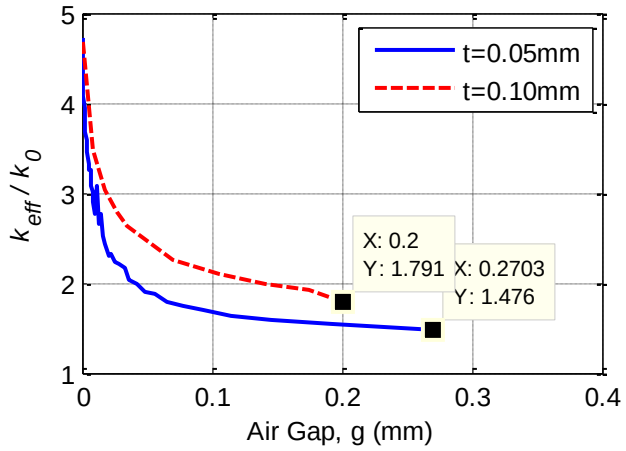

Figure 5 - Propagation constants achievable from the sample transmission line design

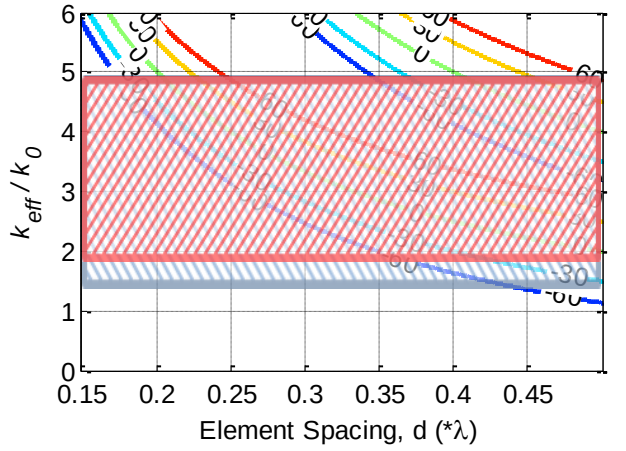

Figure 6 - Achievable scan angles for t=0.05mm (blue) and t=0.10 (red) thick dielectrics.

3. Phased Array as a Circuit

Delivering the correct phase to each element is insufficient to creating a desired pattern; the power delivered to each element must also be considered. For our purposes we decide to deliver equal amplitude to each element. Figure 7 shows the array represented as a circuit. Here, Z is used to denote the element impedance, d the element spacing, k the effective propagation constant, and η the line impedance. This circuit is then collapsed down to the p^{th} element as shown in Figure 8.

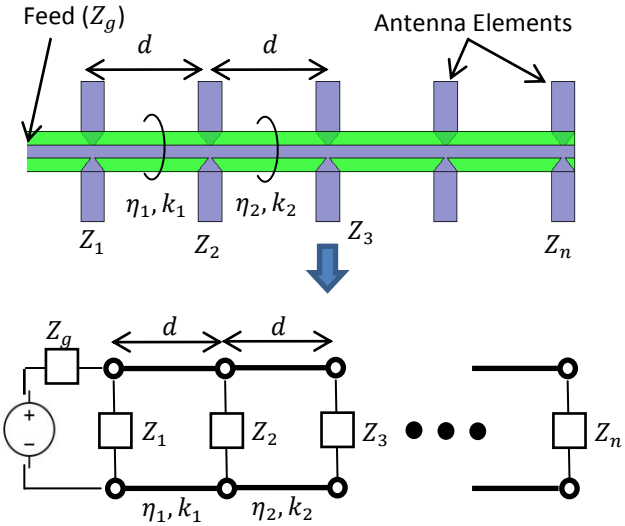

Figure 7 - Schematic and circuit representation of the phased array concept

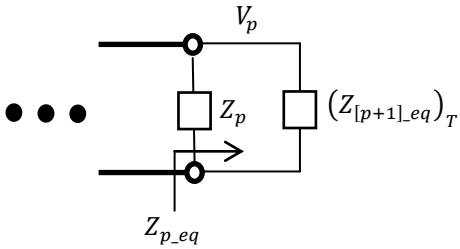

Figure 8 - Equivalent circuit at the p^{th} element in the phased array circuit

For the circuit in Figure 8, Z_p is the impedance of the p^{th} antenna element and V_p is the voltage across the p^{th} antenna element. Since there is one element in the Z_p impedance and $(n-p)$ elements in $(Z_{[p+1]\_eq})_T$ impedance, it follows that

$$(Z_{[p+1]\_eq})_T = \frac{Z_p}{n-p} \quad (1)$$

This insures that power is delivered equally to each element. Using transmission line analysis we find

$$Z_{[p+1]\_eq} = Z_0\left(\frac{\left(Z_{[p+1]\_eq}\right)_T\ cos(kd) - j\eta_p\ sin(kd)}{\eta_p\ cos(kd) - j\left(Z_{[p+1]\_eq}\right)_T\ sin(kd)}\right) \quad (2)$$

Where $Z_{[p+1]\_eq}$ is defined in Figure 9. Combining equations (1) and (2) we find

$$Z_{[p+1]\_eq} = Z_0\left(\frac{\frac{Z_p}{n-p}cos(kd) - j\eta_p\ sin(kd)}{\eta_p\ cos(kd) - j\frac{Z_p}{n-p}sin(kd)}\right) \quad (3)$$

Also we note that

$$Z_{[p+1]\_eq} = Z_{p+1} + \left(Z_{[p+2]\_eq}\right)_T = \frac{Z_{p+1}}{n-p} \quad (4)$$

Now, combining equation (3) and (4)

$$Z_{p+1} = Z_0\left(\frac{Z_p\ cos(kd) - j(n-p)\eta_p\ sin(kd)}{\eta_p\ cos(kd) - j\frac{Z_p}{n-p}sin\ kd}\right) \quad (5)$$

(5) gives the general impedance distribution for uniform excitation.

The array must also be matched to the generator impedance, Z_g. We pick the 0^{th} line impedance (impedance of the line before the first element) equal to the generator impedance $(\eta_0 = Z_g)$. Combining with (5)

$$Z_1 = n\eta_0 \quad (6)$$

An important case to consider is when the same element is used for the entire array;

$$Z_p = Z_{p+1} = Z \quad (7)$$

It follows that

$$\eta_p = \frac{Z}{n-p} \quad (8)$$

This is a condition stating the transmission line impedance must start at a low value as compared to the element impedance and slowly increase. That is, it does not depend on propagation constant or element spacing and thus holds for all scan angles. This can be understood by thinking about a wave propagating down the line. At first, the line and element must be mismatched to allow most of the power to continue on. However, by the end of the line, all of the power must be consumed.

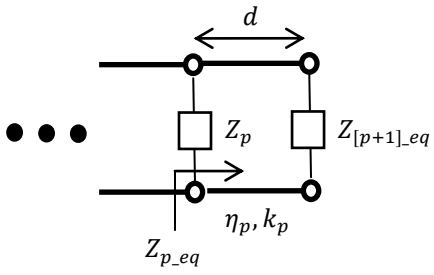

Figure 9 - Equivalent circuit at the $(p+1)$ element in the phased array circuit

4. Array Design

The afore described transmission line design does not have independent impedance and propagation constant control. Thus, the ideal impedance distribution cannot be realized in practice for this design. Nevertheless, the concept is fairly robust and can realize the intended scanning by proper element and transmission line impedance choice. An array, shown in Figure 10, was simulated to display its performance in comparison to an individually fed array.

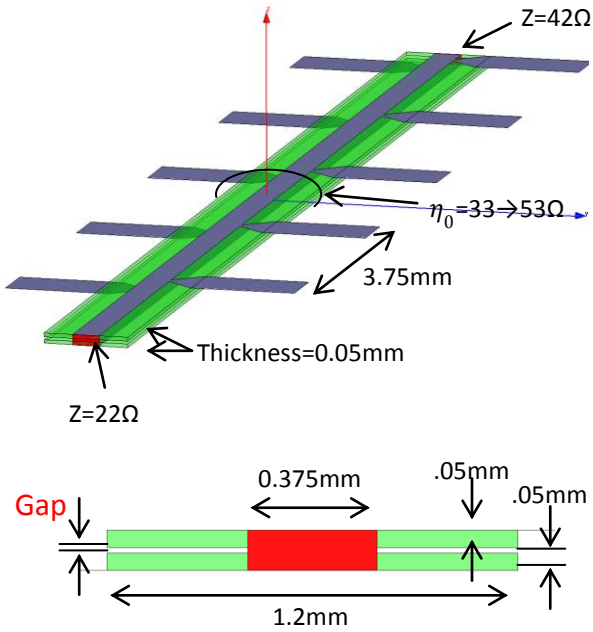

Figure 10 - Five element array using sample transmission line in Figure 4

The transmission line from section II was chosen for the base of this design. A generator impedance of 22Ω was selected to minimize S_{11}, and a termination was added at the end of the line. This termination was used to collect the excess energy left over after radiation from the elements. Without the termination, a second main peak would appear in the opposite direction due to backward propagation of the reflection. Figure 11 shows the simulated performance at -30°, 0°, 30° from boresight in the H-Plane.

It is observed that the performance of our series fed array agrees very well with the individually fed one. One difference is slightly lower gain level. This is due to the energy lost to the termination. With better impedance tapering this difference could be eliminated. The second difference noted relates to the sidelobes. Specifically, we

observe a degraded sidelobe shape due to the infinite bounce between elements disturbing the progressive phase.

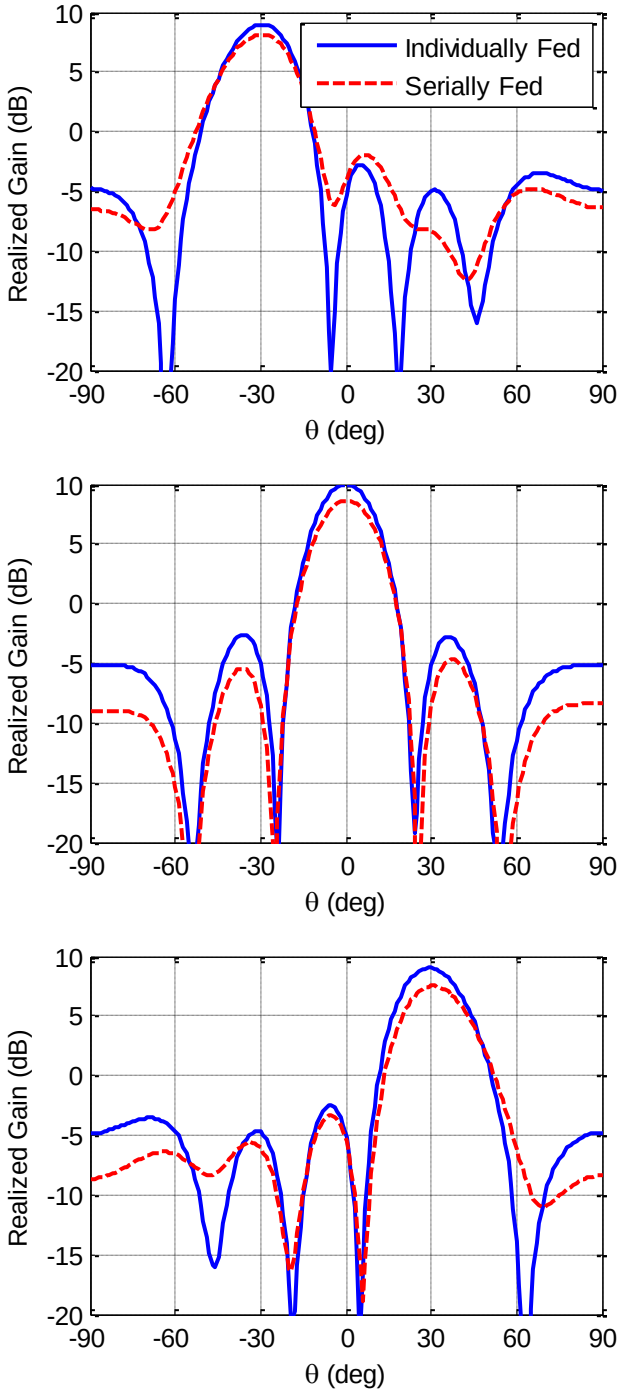

Figure 11 - Simulated array scanning at -30º (top), 0º (middle), 30º (bottom) for individually fed (blue) and series fed arrays (red)

5. Prototype

Our concept becomes more powerful for larger arrays since cost and complexity does not scale with number of elements. For this reason, a large array was chosen to be fabricated and tested. An array of 22 elements (the most to fit on a standard Roger's board) was designed to operate at 13GHz. This array is depicted in Figure 12. A few differences in the transmission line design can be observed. First, the dielectric between the transmission line only appears on one of the plates.

The second change is the addition of two thick pieces of dielectric on the outer surface of the transmission line traces. This was done to ensure structural stability. The dipole impedance was optimized to ensure proper power distribution. With the right choice of element impedance, very good scan patterns were achieved and depicted in Figure 13. However, this particular design was not fabricated in time for inclusion in this paper.

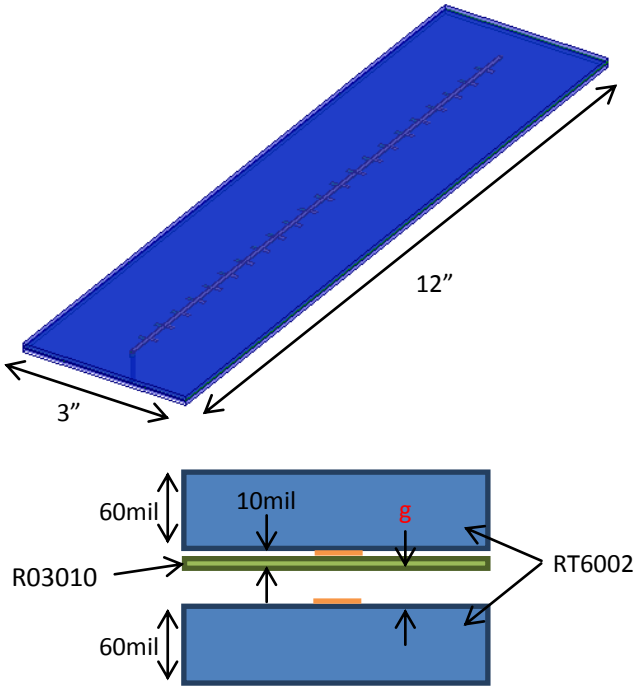

Figure 12 - Design for the prototype full view (top) and cross-sectional view (bottom).

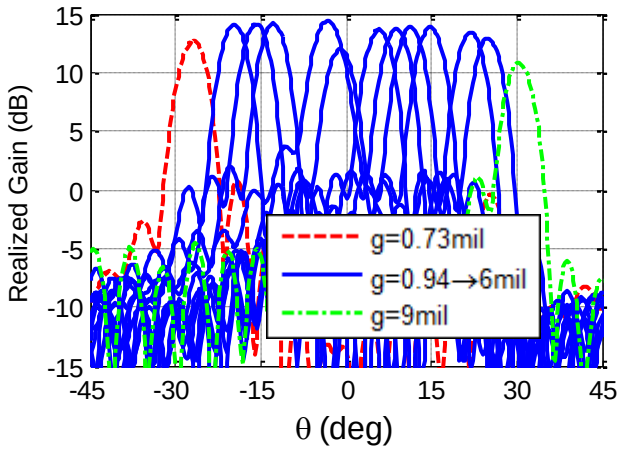

Figure 13 - Scanning patterns as the gap size is changed from g=0.73mil (red) to g=9mil (green)

For demonstration, the same design was built on 120 mil RT6002, seen in Figure 14. Still, the prototype provided good means of validating the concept. The predicted and measured patterns of this prototype are displayed in Figure 15. The first thing to notice is the reduced gain. This is primarily due to our inability to keep the dielectrics flat. Indeed, it is very difficult to maintain board flatness within 0.0003" over a 12"x3" surface. The loss in gain is then the result of the progressive phase lag not being achieved. Consequentially, precise fabrication of the transmission line components is critical for optimal operation of this concept. The second issue is the shifting of the peaks to larger angles. This indicates that the attempt to achieve each air gap, g, yielded larger than expected values. Nevertheless, scanning was realized with the listed differences due to limitations in mechanical adjustment and fabrication. More refined ways of maintaining flatness and gap size are being explored.

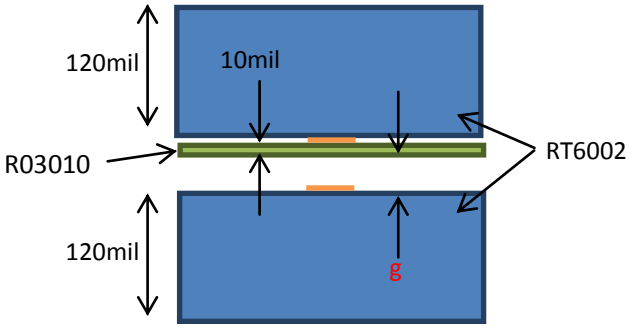

Figure 14 – Transmission line fabricated for validation of the concept

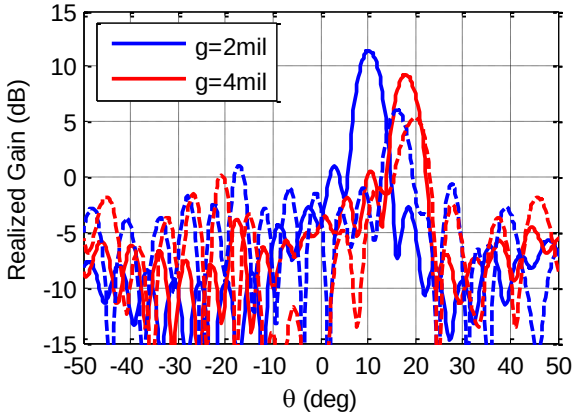

Figure 15 – Simulated (solid) and measured (dotted) prototype scan patterns

6. Summary

A novel array feeding scheme was presented to reduce cost, complexity and weight as compared to traditional phased array feeding techniques. Ideal impedance distributions were also derived to achieve uniform feeding and perfect match at all scan angles. Practical designs were presented which demonstrate comparable performance to individually fed arrays. A prototype was also presented to validate the concept. However, measured results were far from optimal but still showed the ability to scan the beam. Our experimental data reveals that mechanical considerations are of utmost importance to realize this concept.

7. References

[1] Soliman, E.A.; Vasylchenko, A.; Volski, V.; Vandenbosch, G.A.E.; De Raedt, W.; , "Series-fed microstrip antenna arrays operating at 26 GHz," *Antennas and Propagation Society International Symposium (APSURSI), 2010 IEEE* , vol., no., pp.1-4, 11-17 July 2010.

[2] Secmen, M.; Demir, S.; Alatan, L.; Civi, O.A.; Hizal, A.; , "A compact corporate probe fed antenna array," *Antennas and Propagation, 2006. EuCAP 2006. First European Conference on* , vol., no., pp.1-4, 6-10 Nov. 2006.

[3] Mosca, S.; Ciattaglia, M.; , "Ant colony optimization applied to array thinning," *Radar Conference, 2008. RADAR '08. IEEE* , vol., no., pp.1-3, 26-30 May 2008.

[4] Schrank, H.; Schuman, H.; , "Antenna Designer's Notebook-design curves for reducing the number of phase shifters in-phased arrays by subarraying," *Antennas and Propagation Magazine, IEEE* , vol.35, no.2, pp.56-58, April 1993.

[5] Mirzaei, H.; Eleftheriades, G.V.; , "An active artificial transmission line for squint-free series-fed antenna array applications," *Microwave Conference (EuMC), 2011 41st European* , vol., no., pp.503-506, 10-13 Oct. 2011

8. Acknowledgements

This work was supported by a NASA Office of the Chief Technologist's Space Technology Research Fellowship (NSTRF), NASA Grant #NNX11AN16H. A special thanks to Ms. Elizabeth McQuaid and Dr. Kevin Lambert for their help in fabricating and measuring the prototype.